

Task-Modulated Coactivation of Vergence Neural Substrates

Rajbir Jaswal, Suril Gohel, Bharat B. Biswal, and Tara L. Alvarez

Abstract

While functional magnetic resonance imaging (fMRI) has identified which regions of interests (ROIs) are functionally active during a vergence movement (inward or outward eye rotation), task-modulated coactivation between ROIs is less understood. This study tested the following hypotheses: (1) significant task-modulated coactivation would be observed between the frontal eye fields (FEFs), the posterior parietal cortex (PPC), and the cerebellar vermis (CV); (2) significantly more functional activity and task-modulated coactivation would be observed in binocularly normal controls (BNCs) compared with convergence insufficiency (CI) subjects; and (3) after vergence training, the functional activity and task-modulated coactivation would increase in CIs compared with their baseline measurements. A block design of sustained fixation versus vergence eye movements stimulated activity in the FEFs, PPC, and CV. fMRI data from four CI subjects before and after vergence training were compared with seven BNCs. Functional activity was assessed using the blood oxygenation level dependent (BOLD) percent signal change. Task-modulated coactivation was assessed using an ROI-based task-modulated coactivation analysis that revealed significant correlation between the FEF, PPC, and CV ROIs. Prior to vergence training, the CIs had a reduced BOLD percent signal change compared with BNCs for the CV ($p < 0.05$), FEFs, and PPC ($p < 0.01$). The BOLD percent signal change increased within the CV, FEF, and PPC ROIs ($p < 0.001$) as did the task-modulated coactivation between the FEFs and CV as well as the PPC and CV ($p < 0.05$) when comparing the CI pre- and post-training datasets. Results from the Convergence Insufficiency Symptom Survey were correlated to the percent BOLD signal change from the FEFs and CV ($p < 0.05$).

Key words: cerebellar vermis; convergence insufficiency; Convergence Insufficiency Symptom Survey; frontal eye fields; posterior parietal cortex; task-modulated coactivation; vergence

Introduction

DURING ROUTINE DAILY ACTIVITIES, the visual system uses vergence eye movements, which are the inward and outward rotation of the eyes to track objects in three-dimensional space. Several studies support that the posterior parietal cortex (PPC), frontal eye fields (FEFs), and cerebellar vermis (CV) are part of the neural network used to mediate a vergence response (Alkan et al., 2011a, 2011b; Alvarez et al., 2010a, 2010b; Ferraina et al., 2000; Gamlin, 2002; Gamlin and Yoon, 2000; Gamlin et al., 1996; Genovesio and Ferraina, 2004; Gnadt and Mays, 1995; Sakata et al., 1999; Taira et al., 2000). However, patients with the binocular dysfunction known as convergence insufficiency (CI) report asthenopia (visual stress) when engaged in near work such as reading. Symptoms for those with CI include blurred vision, double vision (diplopia), eye strain, reading slowly, and headaches (CITT, 2008; Daum, 1984; Grisham, 1988;

Pickwell and Hampshire, 1981; Scheiman et al., 2009). functional magnetic resonance imaging (fMRI) studies have successfully identified which regions of interests (ROIs) are functionally active during a vergence task (Alkan et al., 2011a, 2011b; Alvarez et al., 2010a). Our prior study had reported a decrease in spatial extent and the correlation of the blood oxygenation level dependent (BOLD) signal with the experimental design for patients with CI compared with binocularly normal controls (BNCs) which increased postvergence training (Alvarez et al., 2010b).

Randomized clinical trials support that repetitive vergence training reduces the visual symptoms of CI patients (Scheiman et al., 2009, 2011) where the reduction of symptoms is sustained 1 year post training (CITT, 2009). Although clinicians commonly prescribe vergence training (also known as vision therapy or orthoptic exercises) to reduce symptoms, the underlying neurophysiological basis for the improvement in symptoms in CI patients is unknown (Cooper and Jamal,

2012; Scheiman et al., 2011). Our prior published study has shown that after vergence training, CI subjects exhibit an increase in the correlation of the experimental design and the BOLD functional activity as well as a significant increase in functional spatial extent within the FEF, PPC, and CV ROIs compared with pretraining measurements (Alvarez et al., 2010b). Yet, studies have not described how ROIs may exhibit task-modulated coactivation within the vergence neural network in BNC and CI subjects before compared with after vergence training. Several types of connectivity analyses have been developed to study the interaction between ROIs (Biswal et al., 1995; Kim and Ogawa, 2012; Margulies et al., 2010).

This study investigated the functional activity and task-modulated coactivation of the neural network used to generate a vergence eye movement. The following hypotheses were tested: (1) significant task-modulated coactivation will be observed between the FEFs, PPC, and CV; (2) significantly more functional activity and task-modulated coactivation will be observed in subjects with normal binocular vision compared with those with the CI; and (3) after repetitive vergence training, the functional activity and task-modulated coactivation will improve in CI subjects compared with each subject's baseline measurements. The aims of this investigation were to study functional activity by analyzing the percent signal change in the fMRI BOLD signal within an ROI and to study task-modulated coactivation by conducting an ROI-based task-modulated coactivation analysis between ROIs in BNC and CI subjects before and after vergence training.

Materials and Methods

Subjects

Seven BNC (three women) and four CI (four women) subjects participated in this study. Subjects had no history of brain disorders and were between the ages of 18 and 35 years. Normal binocular vision was defined as having a normal near point of convergence (NPC) of < 8 cm, assessed by measuring the distance a high acuity target was perceived as

diplopic along the subject's midline (Von Noorden and Campos, 2002), and a normal stereopsis (≤ 50 sec of arc), assessed by the Randot Stereopsis Test (Bernell Corp., South Bend, IN). CI was diagnosed by an optometrist using methods described in our prior study (Alvarez et al., 2010b). The diagnosis criteria comply with conventional clinical methods (Cooper et al., 2011). All subjects signed written informed consent forms approved by the University of Medicine and Dentistry of New Jersey (UMDNJ) and the New Jersey Institute of Technology (NJIT) Institution Review Boards (IRBs) in accordance with the Declaration of Helsinki.

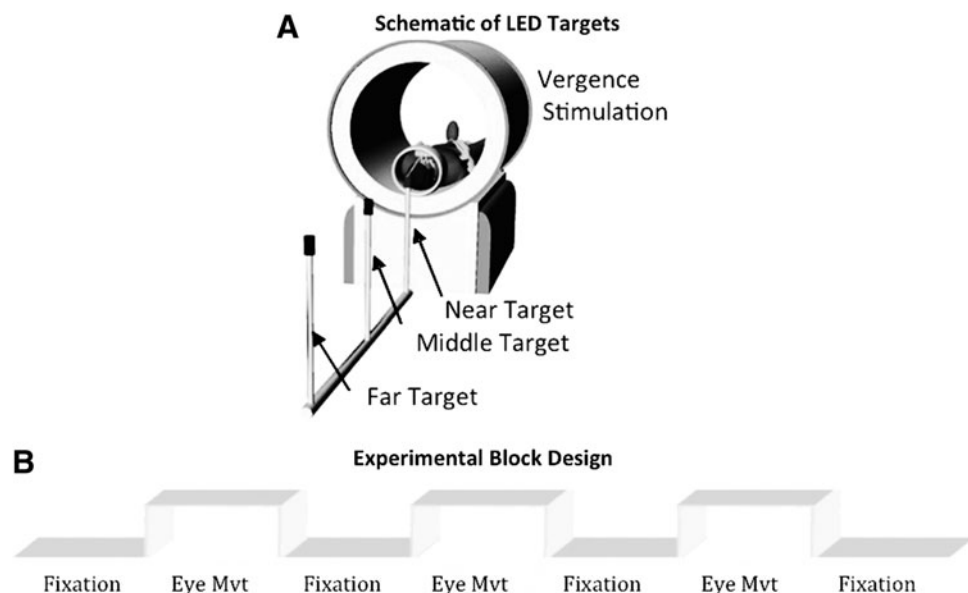
Image instrumentation and acquisition

A 3-Tesla Siemens Allegra Magnetron MRI Scanner with a standard single-channel head coil (Erlangen, Germany) was used to perform the fMRI scans during the experimental tasks. The fMRI imaging parameters used during the acquisition were composed of the following attributes: time of repetition (TR)=2000 msec, time of echo (TE)=27 msec, matrix size=64×64, field of view=220 mm, and flip angle=90°. A total of 32 slices were collected (axial orientation) with a slice thickness of 5 mm. The voxel resolution was 3.4×3.4×5.0 mm³. High-resolution anatomical volumes acquired using a magnetization-prepared rapid acquisition with gradient echo (MPRAGE) were collected after all functional tasks. The MPRAGE imaging parameters included the following attributes: TR=7.2 msec, TE=4.38 msec, T1=900 msec, flip angle=8°, and matrix size=256×256 with a total of 80 acquired slices. The voxel resolution was 0.9×0.9×2.0 mm³. Subjects were instructed to limit head motion and foam padding was used to facilitate the restriction of physical movement. All subjects were positioned supine on the gantry of the scanner with their heads situated along the midline of the coil.

Functional experimental design

The visual stimulus (see Fig. 1A) was carefully aligned with the subject's midline to stimulate symmetrical vergence eye movements to test the hypotheses of this study. Subjects

FIG. 1. (A) Schematic of the LED targets used to stimulate vergence eye movement responses. (B) The experimental block design was composed of sustained fixation (denoted as Fixation) and vergence eye movements (denoted as Eye Mvt) which modulated functional activity of the BOLD signal within the vergence neural substrates. BOLD, bold oxygenation level dependent; LED, light emitting diode.



could see the targets with the aid of a mirror. Visual stimuli were a set of nonferrous light emitting diode (LED) targets that formed a line 5 cm in height by 2 mm in width secured with polyvinyl chloride tubing. The LED stimulus targets were located at the following three vergence demands: 2°, 3°, and 4°. The target positions were chosen because smaller vergence movements have been shown to elicit fewer saccadic responses compared with larger vergence movements (Chen et al., 2010; Coubar and Kapoula, 2008; Semmlow et al., 2008, 2009) as well as due to physical constraints of the scanning room.

The experiment utilized a conventional block design of sustained fixation for the “off” stimulus compared to vergence eye movements for the “on” stimulus as shown in Figure 1B. Prediction is known to decrease the latency and peak vergence velocity of convergence responses (Alvarez et al., 2002, 2005, 2010a; Kumar et al., 2002a, 2002b). Hence, to reduce anticipatory or predictive cues, this experiment utilized a series of vergence eye movements where each target was illuminated for a random amount of time between 3 and 5 sec. LED targets were never simultaneously illuminated. The eye movement sequence illuminated one of the following three stimuli: the near (4°), middle (3°), or far (2°) visual targets where the subject could not anticipate when the next target would illuminate or which of the three targets would be illuminated. Each phase lasted 20 sec and was repeated for 3.5 cycles. Hence, the total experiment time was 2 min 20 sec. The experiment was repeated three times per subject.

Imaging analysis

Image preprocessing. The AFNI (Cox, 1996) and FSL (Jenkinson and Smith, 2001; Jenkinson et al., 2002) software suites were used to process and analyze the raw data retrieved from the MRI scanner. The first five images of each trial dataset were removed to reduce possible T1 stabilization effects, which are commonly performed within fMRI analyses (Biswal et al., 2010).

The AFNI motion correction involves both the removal of spatially coherent signal changes using a partial correlation method, and the application of a six-parameter, rigid-body, least-squares alignment routine. This algorithm estimates for motion artifacts and performs motion correction using six motion parameters. Three parameters calculate the amount (mm) of movement within each plane (anterior to posterior, right to left, and inferior to superior) and three parameters calculate the amount of rotation (°) between planes (yaw, pitch, and roll). These six motion regressors are used within the linear regression model to minimize motion effects of the acquired BOLD signal.

The CompCor component data-driven method was used to reduce the effects of physiological artifacts within the BOLD signal (Behzadi et al., 2007). FSL’s Brain Extraction Tool (BET) (Smith, 2002) function removed nonbrain tissue from the anatomical image dataset. FSLs FMRIBs Automated Segmentation Tool (FAST) (Zhang et al., 2001) stratifies the skull-stripped anatomical dataset into three different segments. Three whole-brain probability maps of each voxel were categorized as the probability of a voxel being cerebral spinal fluid (CSF), WM, or gray matter. The segmented anatomical CSF and WM probability images were transformed

into functional space using FSL’s FLIRT function (Beckmann and Smith, 2004, 2005). To create CSF and WM regressors, CSF and WM probability images were first thresholded using levels of 99% and 97% probability, respectively. Time series from all the voxels surviving the threshold were extracted. The probability levels of this study were more conservative compared with those used previously that used a threshold level of 80% (Biswal et al., 2010). Then, the first five principle components relating to the CSF and WM time series were calculated. FSL’s FEAT command was used to perform the voxel-wise linear regression analysis on all datasets using the 16 aforementioned regressors (six motion parameters, five principle components of CSF, and five principle components of WM). The residuals of the regressed datasets (removal of the 16 artifacts) were then filtered in AFNI using a band-pass filter (full width at half maximum Gaussian filter with cutoff frequencies of 0.01 and 0.15 Hz). The band-pass filter was used to remove direct current offset and high-frequency signals that were probably not neuronal in nature. Thus, the datasets were motion corrected.

A detailed motion analysis of all subjects using a frame displacement method that calculates the absolute value of movement was conducted (Satterthwaite et al., 2013). The average frame displacements with one standard deviation for the degree of rotation were $0.18^\circ \pm 0.07^\circ$, $0.16^\circ \pm 0.09^\circ$, and $0.20^\circ \pm 0.08^\circ$ for yaw, pitch, and roll, respectively. The average frame displacements analyzing all subjects within each plane, with one standard deviation, were 0.36 ± 0.13 , 0.42 ± 0.11 , and 0.37 ± 0.08 mm for the anterior to posterior, left to right, and inferior to superior planes, respectively. No significant differences in motion artifacts were observed between the post- and prevergence training datasets of the CI patients assessed using a paired *t*-test ($p > 0.9$). No significant difference in head motion was observed between the BNC and CI groups ($p > 0.9$). Hence, head motion was not considered problematic within this dataset. Three experimental trials collected in case motion artifact were problematic. A trial that contained considerable motion would be omitted from further analysis. Since our analysis revealed no significant motion artifact, the three experimental trials were averaged per subject after removing the 16 regressors (six motion parameters, five principle components for CSF, and five principle components for WM) from each dataset.

Data analysis. There were two primary image analyses conducted to test the hypotheses of this study: (1) the average percent signal change per subject within each ROI assessed the functional activity within an ROI and (2) an ROI-based correlation technique of the average ROI time series to assess the task-modulated coactivation between ROIs.

Regions of interest. The ROIs were defined using anatomical markers coupled with a model-driven method to identify functional activity near the anatomical markers. Neurophysiology studies on primates support that the following ROIs are involved in vergence eye movements: FEFs, PPC, and CV (Gamlin and Yoon, 2000; Gamlin et al., 1996). This experiment sought to stimulate the cortical and cerebellar regions required to mediate vergence eye movements.

The following ROIs were drawn in native space using anatomical and functional markers: FEFs, PPC, and CV. The bilateral FEFs were defined as the area within the intersection

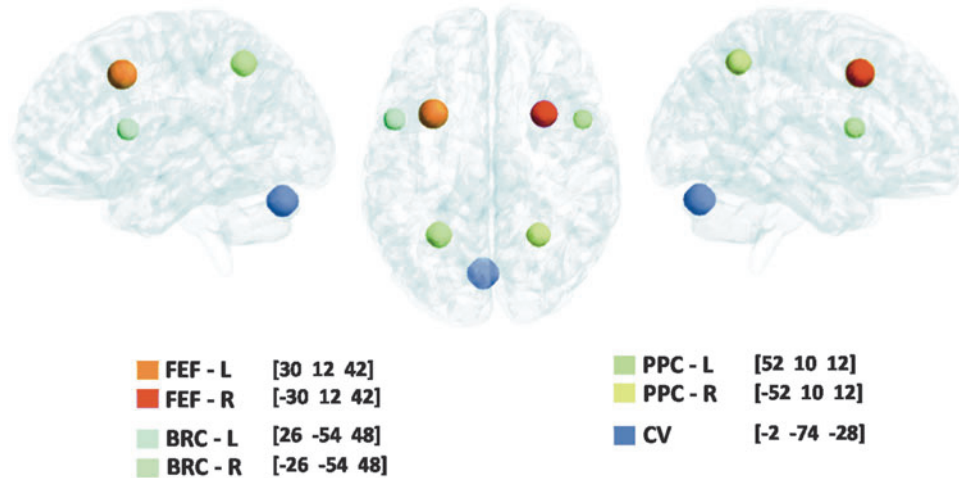


FIG. 2. Representation of average masks with one standard deviation for the frontal eye fields, left and right (FEF-L [brown] and FEF-R [red]), posterior parietal cortex, left and right (PPC-L [dark green] and PPC-R [yellow]), Broca's region, left and right (BRC-L [light blue] and BRC-R [light green]), and cerebellar vermis (CV [dark blue]) shown using three views within a three-dimensional model brain. The centroid of each mask is denoted as left (positive) or right (negative), anterior (positive) or posterior (negative), and superior (positive) or inferior (negative).

between the precentral sulcus and superior frontal sulcus. The PPC was within the vicinity of the intraparietal sulcus. The CV regions VI and VII were defined on the mid-sagittal plane. Broca's region served as a control ROI because it was not stimulated in prior fMRI vergence studies (Alkan et al., 2011a, 2011b; Alvarez et al., 2010a). The mask for Broca's region was created using only anatomical markers that were defined near the inferior frontal gyrus anterior to the motor strip. Figure 2 depicts the ROIs within a three-dimensional brain model used in this study that were identified using axial slices. Table 1 lists the volume of each subject's masks for FEF-L (left), FEF-R (right), PPC-L, PPC-R, CV, Broca-L, and Broca-R. The average and standard deviation for the masks used are also listed in Table 1. The averages with one standard deviation of each ROI are shown in Figure 2. As Figure 2 shows, none of the masks overlap to avoid any

partial-volume effects. The centroid of the mask listed as left (positive) or right (negative), anterior (positive) or posterior (negative), and superior (positive) or inferior (negative) is denoted within the legend of Figure 2.

A general linear model using a reference time series representation of the block design experimental stimulus that convolved with the hemodynamic response function was used. Correlation maps were created using a threshold of $r \geq 0.4$ ($p < 0.05$) to show active brain regions. Mask identification was facilitated by observing the active brain regions coupled with the anatomical locations described earlier for the FEFs, PPC, and CV. Broca's region was the control ROI and was identified strictly using anatomical markers. Since the datasets were not transformed into a standardized space such as the Montreal Neurological Institute (MNI) space, some variance is also observed for the mask of Broca's region.

TABLE 1. VOLUME OF EACH MASK MEASURED WITHIN EACH INDIVIDUAL SUBJECT'S NATIVE SPACE IN mm^3

Volume (mm^3)	FEF-L	FEF-R	PPC-L	PPC-R	CV	Broca-L	Broca-R
HC 1	867	809.2	1271.6	1098.2	982.6	520.2	520.2
HC 2	809.2	751.4	1271.6	1098.2	1213.8	520.2	520.2
HC 3	1040.4	867	1445	982.6	1040.4	520.2	520.2
HC 4	809.2	1098.2	1502.8	965.2	867	520.2	520.2
HC 5	751.4	924.8	1693.6	1734	1040.4	520.2	635.8
HC 6	1156	924.8	1676.2	1734	1156	346.8	635.8
HC 7	809.2	924.8	1676.2	1734	982.6	520.2	520.2
CI 1	895.9	982.6	953.7	751.4	953.7	520.2	520.2
CI 2	809.2	1098.2	1213.8	693.6	867	520.2	520.2
CI 3	867	809.2	1849.6	1069.3	1156	433.5	520.2
CI 4	867	722.5	1184.9	1271.6	809.2	549.1	520.2
Average	880	901	1430	1194	1006	499	541
Standard deviation	118	126	275	382	131	58	47

FEF-L, FEF-R, PPC-L, PPC-R, and CV used both anatomical markers and functional activity to define the mask. Broca-L and Broca-R used only anatomical markers to serve as a control ROI to study the variability within a nonstimulated ROI.

Broca, Broca's region; CI, convergence insufficiency; CV, cerebellar vermis; FEF, frontal eye field; HC, healthy control; L, left; R, right; PPC, posterior parietal cortex; ROIs, regions of interests.

Broca's region served as a control ROI (not related to the hypotheses of this study). Language was not manipulated within the experimental protocol. Prior investigations show that Broca's region was stimulated during experiments that study language (Geschwind, 1970; Kim et al., 1997) but was not stimulated within vergence eye movement experiments (Alkan et al., 2011a, 2011b). Hence, Broca's region was used as a control ROI to study the variability within a nonstimulated ROI. The Broca mask only used anatomical markers to pool the time series from that region since the BOLD signal did not significantly correlate to the experimental design.

Functional activity analysis. All data were kept in native space (i.e., data were not transformed into Talairach & Tournoux or MNI space) to reduce any warping artifacts. The time series located within the vicinity of the anatomical markers, which had a Pearson correlation coefficient of $r \geq 0.4$ ($p < 0.05$) with the hemodynamic model described earlier, were pooled. This study used a within-subject longitudinal design. The same threshold was used on the pre- and postvergence training analyses. Hence, we assume that any potential differences observed within the datasets were due to training. The BOLD percent signal change for each ROI per subject comparing elevated activation observed during the vergence task to the baseline of sustained fixation was computed from the time series. The individual-subject percent signal change values were pooled to conduct the group-level statistical analysis described within the statistical analyses section. The time series from each ROI were also correlated with the square wave experimental block design to compute Pearson correlation values.

Task-modulated coactivation analysis. Using the averaged signal from each ROI described previously, a task-modulated coactivation analysis was conducted. A pair-wise correlation was computed using the averaged time series for each ROI per individual subject. The MATLAB software suite (Waltham, MA) was used to perform a pair-wise linear correlation analysis between the following seven ROIs: left and right frontal eye field (FEF-L and FEF-R), left and right posterior parietal cortex (PPC-L and PPC-R), cerebellar vermis VI and VII (CV), and left and right Broca's region (Broca-L and Broca-R). This analysis was conducted on the seven BNCs and the four CI subjects before and after vergence training. These data were then pooled to conduct a group-level analysis. A correlation matrix was plotted using the mean values from each of the three groups studied (BNC, CI before, and CI after vergence training).

Vergence training protocol for CI subjects. Repetitive vergence training was utilized to provoke changes in the neural substrates that stimulate vergence eye movement responses. The CI subjects participated in a total of 18 h of vergence training: 6 h at home and 12 h in the laboratory. Home training was monitored by having each CI subject recorded in a log book the amount of time spent on vergence training. It entailed two 10-min sessions (morning and evening) 3 days per week for 6 weeks. Laboratory training was composed of 1-h sessions, twice per week for 6 weeks. Within a single day, a subject participated in either laboratory or home training but not both. Details of the vergence

training were described in our previous publication (Alvarez et al., 2010b). The laboratory and home training consisted of step and ramp stimuli similar to methods used clinically (Griffin, 1988; Scheiman and Wick, 2008).

CI subject symptoms. Symptoms were quantified using the Convergence Insufficiency Symptom Survey (CISS), which is a 15-question survey (CITT, 2008). Each symptom is scored from zero to four where zero represents the symptom never occurs and four represents the symptom occurs very often. The responses are summed where a score of 21 or higher has been validated to have a sensitivity of 98% and specificity of 87% in young adults between 18 and 35 years of age (Rouse et al., 2004).

Statistical analyses. The subject data were stratified into the following three groups: BNCs, CI subjects before vergence training, and CI subjects after vergence training. An unpaired *t*-test was used to determine whether significant differences were observed in (1) the percent signal change of the BOLD fMRI signal within an ROI and (2) the task-modulated coactivation between ROIs by comparing the CI and the BNC groups. A paired *t*-test determined whether the CI subjects exhibited significant changes in the percent signal change of the fMRI BOLD signal within an ROI, task-modulated coactivation between ROIs, CISS, NPC, vergence ranges, and near dissociated phoria, for the postvergence training measurements compared with pretraining measurements. Linear regression was conducted between (1) the CISS and the BOLD percent signal change and (2) the CISS and the task-modulated coactivation where the Pearson correlation coefficient was assessed for significant correlation. Statistics were calculated using NCSS2004 (Kaysville, UT). Significance was defined as a *p*-value < 0.05 . Bonferroni correction was not applied because of the limited number of subjects within the study. Figures were generated using MATLAB (Mathworks, Natick, MA).

Results

Clinical vision parameters

A paired *t*-test revealed a significant difference comparing the baseline (before vergence training) parameters and the after vergence training parameters for the following measurements: the NPC ($t = 4.9$; $p = 0.04$), base out positive fusional vergence range ($t = 9.5$; $p = 0.01$), near dissociated phoria ($t = 11$; $p = 0.008$), and CISS ($t = 3.6$; $p = 0.05$). All significant changes are improvements to the clinical signs and symptoms studied.

Typical functional activity and task-modulated coactivation from a BNC and a CI before and after vergence training

Figure 3 shows data from two subjects whose individual parameters were most similar to the group averages, one BNC (left column), one CI subject before vergence training (middle column), and the same CI subject after vergence training (right column). Figure 3A shows the average time series from the FEF-L (red line) and the PPC-L (green line) plotting the percent signal change as a function of volumes collected (a total of 70 volumes equating to 140 sec in

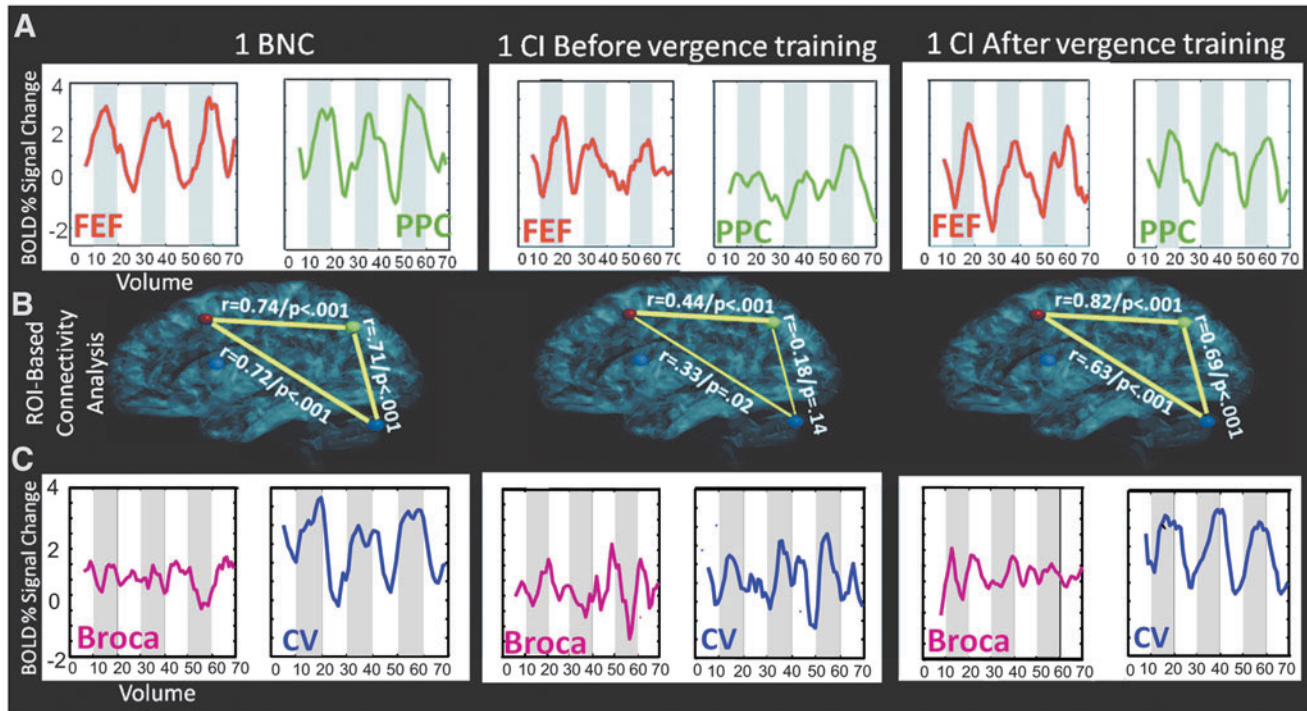


FIG. 3. (A) Averaged time series for the FEF-L (red) and PPC-L (green) ROIs from one typical BNC (left) and one CI before (middle) and the same CI after vergence training (right). (B) Example of the task-modulated coactivation analysis between FEF-L (red circle), PPC-L (green circle), CV (blue circle), and Broca-L (purple circle). The Pearson correlation coefficient (r -value) and p -value are shown where the thickness of the line represents the significance. The time series from Broca-L was not significantly correlated to FEF-L, PPC-L, or CV in any of the subjects studied. (C) Averaged time series for Broca-L (purple) and CV (blue). BNC, binocularly normal control; CI, convergence insufficiency; ROIs, regions of interests.

duration). The thickness or absence of a yellow line between ROIs in Figure 3B represents the strength and significance of the task-modulated coactivation. Each line is labeled with the Pearson correlation coefficient and p -value was derived from the correlation between the following ROIs: FEF-L, PPC-L, Broca-L, and the CV denoted as red, green, purple, and blue circles, respectively. Note, Broca-L has no lines to the FEF-L, PPC-L, and CV because the task-modulated coactivation was not significant ($p > 0.1$) in these two subjects shown or in any of the other subjects analyzed. Figure 3C shows the time series from Broca-L (purple lines) and from the CV (blue lines). The BNC has an FEF time series that is more correlated ($r = 0.66$; $p < 0.001$) with the experimental block design (white and gray boxes for the 3.5 cycles of the experiment) compared with the CI before vergence training ($r = 0.33$; $p < 0.01$). After vergence training, this subject's FEF correlation with the block design increases ($r = 0.73$; $p < 0.001$). Similar trends are observed for the PPC and the CV. As expected, the time series from Broca's region (control ROI to study variability of a nonstimulated region) does not correlate with the experimental block design for the BNC and the CI before or after vergence training ($r = 0.15 \pm 0.05$; $p > 0.1$).

Figure 3B shows the ROI-based task-modulated coactivation analysis for two individual subjects, one BNC and one CI before and the same CI after training. The average time series were significantly correlated between the FEFs and PPC, FEFs and CV, and PPC and CV for the BNC ($r > 0.71$;

$p < 0.001$). However for the BNC, the time series from Broca's region was not significantly correlated to FEFs, PPC, or CV, displayed without a line between Broca's region (purple circle) and the other ROIs ($r < 0.1$; $p > 0.2$). Figure 3B shows the data from CI subject 3, who had the highest task-modulated coactivation within the CI group before vergence training. Even for this CI subject (before training), the task-modulated coactivation ($0.18 < r < 0.44$) was less compared with the BNC subjects. For this same CI subject after vergence training, the correlations between the FEFs, PPC, and CV improved ($r > 0.63$; $p < 0.001$) compared with the baseline measurements. For the CI subject before and after vergence training, the time series from Broca's region did not correlate to any of the other ROIs ($r < 0.2$; $p > 0.1$). The width of the yellow line represents the level of significance. High significance ($p < 0.001$) is denoted using a thick line and lower significance ($0.001 < p < 0.05$) is denoted using a thin line.

Group-level analysis of functional activity

Figure 4 shows the average with one standard deviation for the group-level analysis of the percent change in the BOLD signal per ROI for the following groups: BNCs (green bar), CI subjects before vergence training (blue bar), and CI subjects after vergence training (red bar). When comparing the BNC to the CI data before vergence training using an unpaired t -test, significant differences were observed within the FEFs, PPC, and CV ($t > 2.3$;

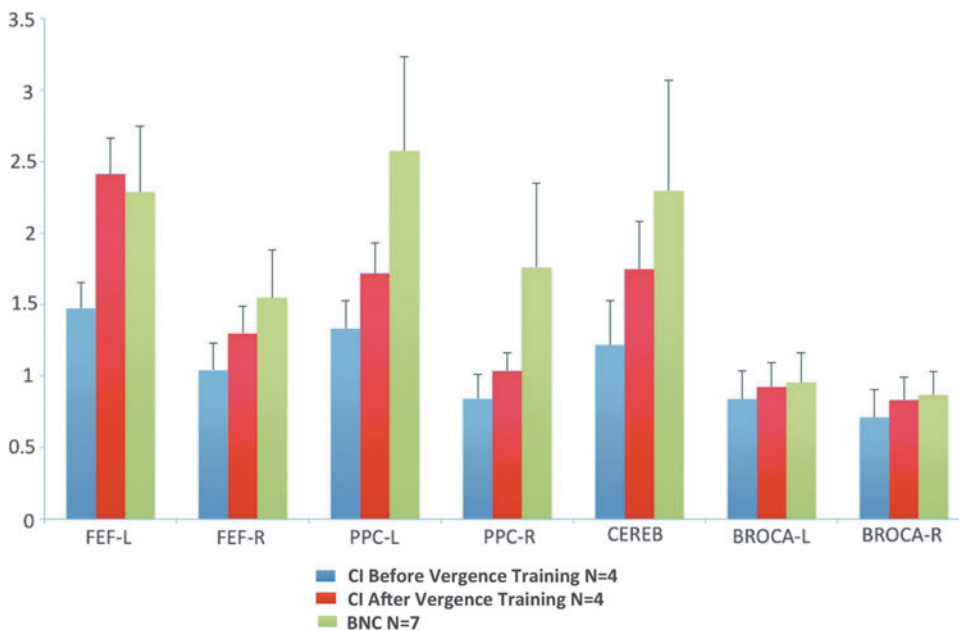


FIG. 4. Percent BOLD signal change for FEF-L (left), FEF-R (right), PPC-L, PPC-R, CV, Broca-L, and Broca-R for CI subjects before vergence training (blue), CI subjects after vergence training (red), and the BNC subjects (green). Bar plots are the average plus one standard deviation. Color images available online at www.liebertpub.com/brain

$p < 0.05$). Significant differences were not observed within Broca's region between the BNC and either the before or after vergence training CI datasets ($t > 1.1$; $p > 0.3$). A paired t -test showed that the percent change in the BOLD signal in the FEFs, PPC, and CV of the four CI subjects who participated in vergence training was significantly greater after training compared with the baseline values ($t > 2.6$; $p < 0.001$). No statistical difference was observed in Broca's region ($t = 1.2$; $p > 0.3$) when comparing the baseline and after vergence training data.

Group-level analysis of task-modulated coactivation

Figure 5A shows a correlation matrix of the group-level BNC dataset. The color bar represents the average correlation between the ROIs labeled in the row versus the column. In the BNC group, strong correlations were observed between the left and right FEFs, left and right PPC, and the CV. The time series from Broca's region were not significantly correlated to the FEFs, PPC, or CV ($r < 0.2$; $p > 0.1$). Figure 5B and 5C shows a correlation matrix for the group-level CI dataset before and after vergence training, respectively. For the CI subjects, correlation values between the FEFs, PPC, and CV were lower before vergence training and these values increased postvergence training. Figure 5 plots D through F display the p -values for the following statistical comparisons that were conducted: unpaired t -test comparing BNC versus the CI before vergence training datasets, an unpaired t -test comparing the BNC and the CI after vergence training datasets, and a paired t -test comparing the CI before and after training datasets. The task-modulated coactivation of the BNC group was significantly different compared with the task-modulated coactivation of the CI group before vergence training dataset for the FEFs, PPC, and CV. After vergence training, the CI group dataset was not significantly different compared with the task-modulated coactivation of BNC group dataset. The paired t -test comparing the before and after vergence training CI datasets revealed that a significant increase of task-modulated coactivation

was observed between the FEF-L and CV as well as the PPC-L and CV ($p < 0.05$).

The linear regression analyses reported that for the CI datasets, the CISS and the percent BOLD signal change from the following ROIs FEF-L (Fig. 6A), FEF-R (Fig. 6B), and CV (Fig. 6C) were significantly correlated ($r \leq -0.7$; $p < 0.02$). The correlations between CISS and the following ROIs PPC-L, PPC-R, Broca-L, and Broca-R were not significant ($-0.6 \leq r \leq 0.4$; $p > 0.1$). Linear regression analyses were also conducted on the differences between the percent change in the BOLD signal as a function of the differences in the CISS. Difference was defined as the measurements after vergence training minus the initial measurements before vergence training. The sample size is small where none of the correlations were significant ($p > 0.1$). However, the correlation for the difference in the BOLD percent signal change for the cerebellum ROI as a function of the difference in CISS had a Pearson correlation coefficient of $r = 0.8$. Linear regression analyses were also conducted to assess the correlation between the task-modulated coactivation and the CISS. Significant correlations between the task-modulated coactivation of each pair of ROIs and the CISS were not observed ($-0.6 \leq r \leq 0.4$; $p > 0.05$). The greatest correlation was observed between the CISS and the task-modulated coactivation between the right FEFs and left PPC ($r = -0.65$; $p = 0.08$).

Discussion

The data support the hypotheses that were tested. Significant task-modulated coactivation was observed between the FEFs, PPC, and CV ($p < 0.05$) in BNC subjects. Functional activity and task-modulated coactivation studying the FEFs, PPC, and CV assessed via the percent BOLD signal change and an ROI-based correlation analysis, respectively, was reduced in CI subjects before vergence training compared with BNCs. After vergence training, both functional activity and task-modulated coactivation between the FEFs, PPC,

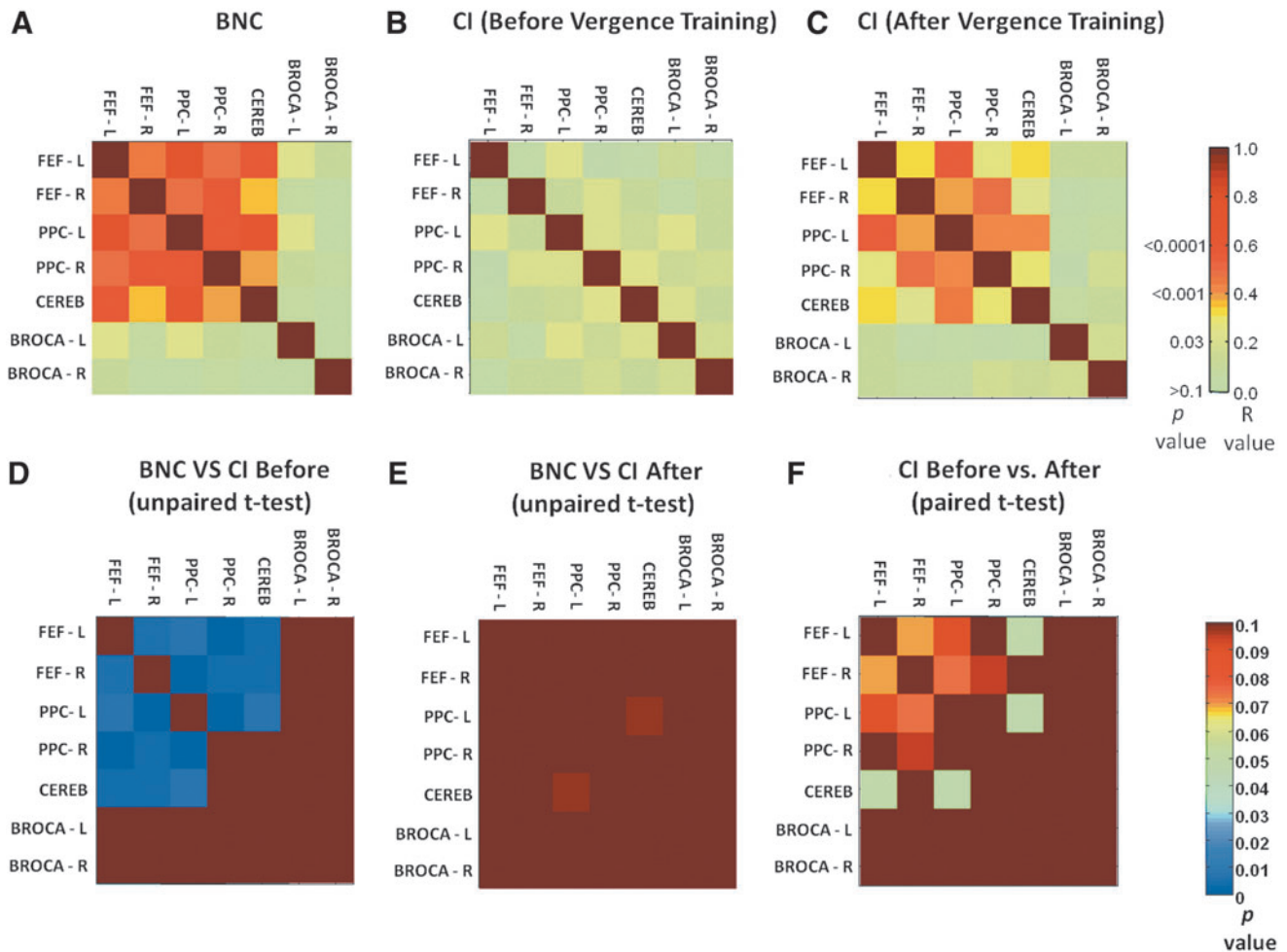


FIG. 5. Pair-wise correlation analyses. Group-level correlation values are between FEFs (left and right), PPC (left and right), CV, and Broca's region (left and right) for BNCs (**A**); CI subjects before vergence training (**B**); and the same CI subjects after vergence training (**C**). Group-level statistical comparisons reporting p -values are shown for BNC versus CI before vergence training (**D**), BNC versus CI after vergence training (**E**), and CI before versus CI after vergence training (**F**).

and CV significantly increased in CI subjects. Broca's region was not significantly different between the BNC and the CI subjects (using either the before or after training data). The results of this study will be compared with those in the literature.

Functional activity within an ROI

Nonhuman primate single-cell electrophysiology studies have investigated the influence of disparity in FEFs using symmetrical step stimuli (Gamlin and Yoon, 2000), near and far targets (Ferraina et al., 2000), and smooth sinusoidal tracking stimuli (Akao et al., 2005; Fukushima et al., 2002). The FEFs and PPC have also been shown to be involved in predictive oculomotor learning (Tseng et al., 2013). The PPC encodes for different binocular distances defined by different vergence angles studying primates using single-cell recordings (Breveglieri et al., 2012; Ferraina et al., 2009; Genovesio and Ferraina, 2004) and humans using transcranial magnetic stimulation (Kapoula et al., 2001, 2004, 2005; Yang and Kapoula, 2004) and fMRI (Alvarez et al., 2010a; Alkan et al., 2011a, 2011b; Quinlan and Culham, 2007). Primate single-cell studies have also shown that the

CV is used to mediate a vergence response (Gamlin et al., 1996; Nitta et al., 2008a, 2008b). Patients, particularly those with lesions to the cerebellar vermal regions, exhibit a decrease in slow tracking vergence (Sander et al., 2009).

This present study further confirms that the FEFs, PPC, and CV are metabolically active during a vergence task. The novelty of this study's results is that the functional activity of the FEFs, PPC, and CV are reduced in CI subjects at baseline compared with BNC subjects and significantly improved after 18 h of vergence training to levels more similar to those exhibited by the BNC subjects. The results support the hypotheses that subjects with CI have reduced functional activity compared with BNCs and that after vergence training the functional activity improves to levels more similar to those observed in BNCs.

Task-modulated coactivation between ROIs

The task-modulated coactivation of the vergence network is not completely understood. Neurophysiology studies on primates support a direct connection between the FEFs and PPC as well as a connection between the FEFs and cerebellar

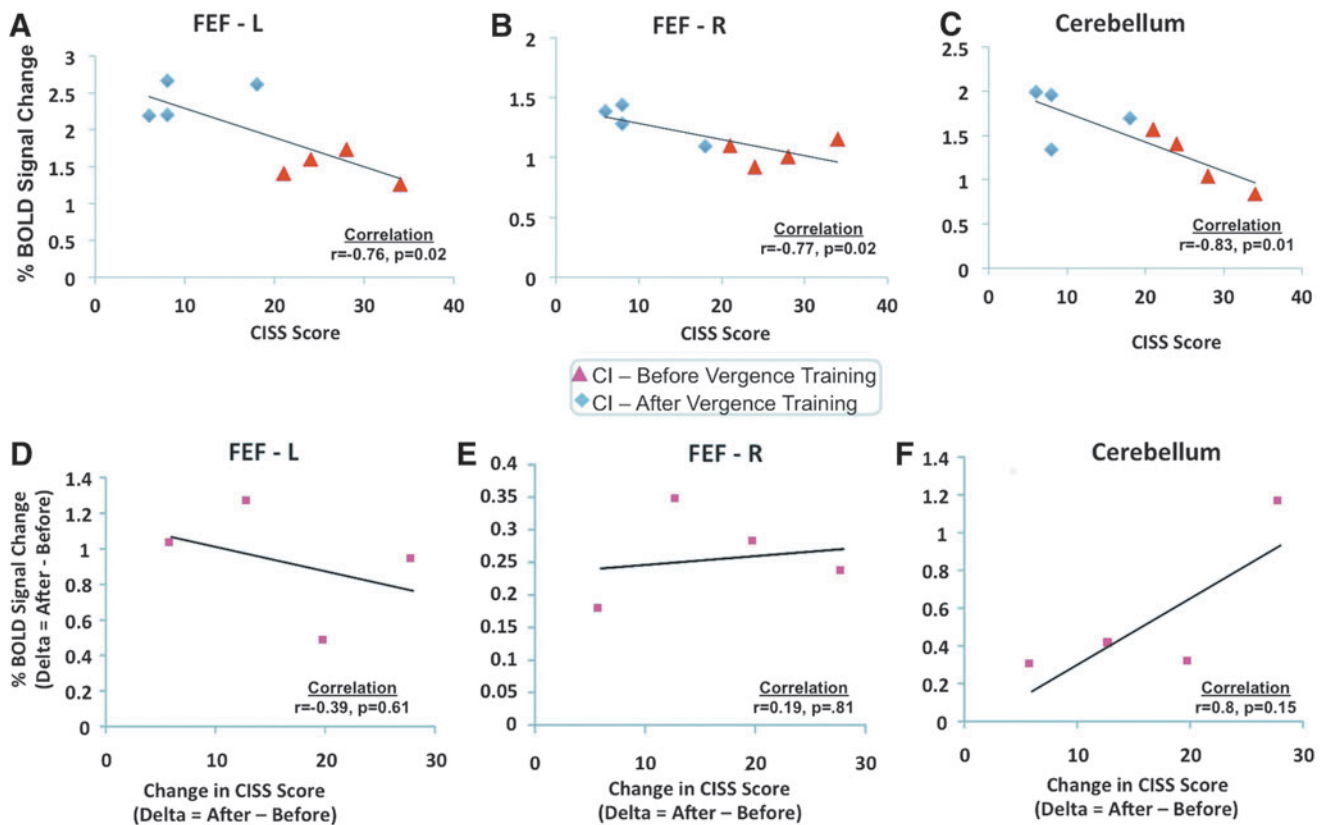


FIG. 6. Percent BOLD signal change versus CISS scores for CI groups (before and after vergence training) for the FEF-L (A), FEF-R (B), and cerebellar vermis (CV) (C). Linear regression analyses for the difference in the percent BOLD signal change (measurements after vergence training minus measurements before vergence training) as a function of the change in the CISS score (after minus before vergence training) for the FEF-L (D), FEF-R (E), and cerebellum (F). CISS, Convergence Insufficiency Symptom Survey. Color images available online at www.liebertpub.com/brain

cortex through the nucleus reticularis tegmenti pontis (Gamlin, 2002). Functional connectivity studies using resting-state fMRI support connectivity between the FEFs and PPC studying humans and primates (Hutchison et al., 2012). In addition, direct connections between the lateral intraparietal area and the oculomotor cerebellum have been identified using a combination of rabies virus and a conventional cholera toxin B tracer in nonhuman primates (Prevosto et al., 2010). The present study implies that the FEFs, PPC, and CV may have functional connections quantified through the task-modulated coactivation analysis.

Information is scarce in terms of how task-modulated coactivation may be altered for those with CI. This present study supports the hypothesis that the task-modulated coactivation of CI subjects is on average significantly lower compared with task-modulated coactivation observed within BNC subjects. However, after 18 h of vergence training, CI patients exhibited significant correlation between the FEF, PPC, and CV ROIs showing task-modulated coactivation patterns more similar to BNC subjects thus supporting the third hypothesis. These data suggest that vergence training not only increases the percent BOLD signal change within the FEFs, PPC, and CV but also increases the task-modulated coactivation between the FEF and CV as well as the PPC and CV ROIs. Increasing the correlation of the BOLD signal within and between the FEFs, PPC, and CV may be one

mechanism that leads to the sustained reduction in visual symptoms that CI subjects experiences after vergence training. These data support that the CISS was significantly correlated to the BOLD percent signal change within the FEFs and CV. These data suggest that future therapeutic interventions may consider targeting the improvement of the metabolic activity within FEFs and CV.

Clinical relevance

The techniques developed within this study can serve to compare different vergence training protocols to provide a deeper understanding of the mechanisms evoked during vergence training and serve to compare future vergence training protocols. Ultimately, the techniques within this study have the potential to evaluate the efficacy of different therapeutic protocols leading to further improvements in vision function.

Rehabilitation studies

While eye movement rehabilitation studies that utilize fMRI are scarce, fMRI has been used to study the effects of rehabilitative training tasks that use eye movements such as reading (Laatsch and Krisky, 2006; Laatsch et al., 2004; Shaywitz et al., 2003). One study investigated a saccadic task and reading comprehension task before and after cognitive rehabilitation therapy where functional activity increased post

therapy compared with the baseline measurements studying patients with mild (Laatsch et al., 2004) and severe (Laatsch and Krisky, 2006) traumatic brain injury. Reading investigations in dyslexic patients showed reduced activation in the left parietotemporal and occipitotemporal regions in patients who did not improve their reading ability compared with dyslexic patients who did improve their reading in adulthood (Shaywitz et al., 2003). Another study on vision-restoration training has shown an increase in visual receptive fields correlated to an increase in the amplitude of the BOLD signal in patients with cerebral blindness (Raemaekers et al., 2011). Similar to the prior reading, saccade and vision-restoration training protocols, this current study also reports an increase in functional activity assessed via the BOLD percent signal change compared with each subject's baseline measurements.

Functional connectivity has become more common within longitudinal studies to investigate whether the interaction between ROIs is an independent factor that may contribute to the sustained improvement observed in rehabilitation. The present study was novel because it was the first to analyze task-modulated coactivation for those with CI undergoing repetitive vergence training. For brain injury patients, studies have shown a decrease in functional connectivity 3 months postinjury compared with neurologically normal subjects where functional connectivity improved to levels more similar to controls 6 months postinjury (Nakamura et al., 2009). For patients with multiple sclerosis, the increase in functional connectivity assessed as an increase in correlation between ROIs predicted the effects of cognitive rehabilitation quantified via assessment of attention, executive function, depression, and quality of life (Parisi et al., 2013) as did another study that used the modified Story Memory Technique (Leavitt et al., 2012). Patients with stroke also exhibited a decrease in functional activity poststroke (within the first month) and connectivity was improved postrehabilitation where functional connectivity was significantly correlated to motor function (Golestani et al., 2013; Park et al., 2011). For healthy individuals, learning a novel motor task resulted in an increase in functional connectivity within the fronto-parietal network after repetitive training of the motor task (Taubert et al., 2011). In summary, prior rehabilitative interventions in those with brain injury, stroke, and multiple sclerosis all report that an increase in functional connectivity is correlated to an improvement in behavioral function. Similar to the aforementioned functional connectivity studies, this current study supports that an increase in task-modulated coactivation after 18 h of vergence training was observed compared with baseline measurements in CI subjects.

Reliability of fMRI

When studying sensory, motor, and cognitive function, several fMRI investigations conclude that fMRI has high test-retest precision (Brannen et al., 2001; Freyer et al., 2009; Gamlin et al., 1996; Kiehl and Liddle, 2003; Loubinoux et al., 2001; Peelen and Downing, 2005; Specht et al., 2003; Yetkin et al., 1996; Yoo et al., 2005; Zou et al., 2005). Similar results are reported for resting-state fMRI studies (Blautzik et al., 2012; Meindl et al., 2010; Shehzad et al., 2009; Song et al., 2012). A recent eye movement study of the reliability of a saccadic task showed an interclass correlation coefficient of >0.5 in 75% of the subjects

studied (Ming et al., 2012). Further, studies report that reliability is improved when movement artifacts are small (Lund et al., 2005) and that 3-T scanners have better repeatability compared with 1.5-T scanners (Zou et al., 2005).

Study limitations and future direction

This study has a small sample size and future studies should evaluate whether the results observed here generalize to a larger population. It is unknown whether the changes observed immediately after therapy persist long term. We would anticipate that the observed functional changes would be sustained because a randomized clinical trial that studied CI patients reports that the reduction in CISS continues one year postvergence training (CITT, 2009). Ideally, future studies will include a larger scale randomized clinical trial composed of four groups. Half of the subjects would be BNCs and the other half would have CI. Half the BNC and half of the CI subjects would participate in active vergence training while the remaining BNC and CI subjects would receive placebo training. This type of study is beyond the resources of this present study.

While the present study used Broca's region as a control ROI to study the variability within fMRI, future studies should also assess the repeatability of functional activity stimulated with vergence eye movements within BNC subjects. A repeatability investigation of functional activity evoked from saccadic eye movements using 45 subjects reports activation consistency between 60% and 85% within the same subject (Lukasova et al., 2013). Hence, we suspect that the test-retest analysis of vergence will be similar to that observed within saccadic studies.

Conclusions

The data of the present study support that CI subjects had a decrease within the percent BOLD signal change within the FEFs, PPC, and CV compared with BNC subjects, which improved to levels more similar to BNC subjects after 18 h of vergence training. The task-modulated coactivation between the FEFs, PPC, and CV was also reduced in CI patients compared with BNCs and improved postvergence training. The CISS was significantly correlated to the BOLD percent signal change within the FEFs and CV. Results support the following: (1) an increase in functional activity within ROIs and (2) task-modulated coactivation between the FEF, PPC, and CV ROIs may in part lead to the sustained reduction in symptoms assessed via the CISS reported by CI subjects.

Acknowledgments

This research was supported in part by NSF MRI CBET1228254 and NIH EY02326 to T.L.A. and NIH AG032088R0 to B.B.B.

Author Disclosure Statement

All authors have no competing financial interests.

References

- Akao T, Kurkin SA, Fukushima J, Fukushima K. 2005. Visual and vergence eye movement-related responses of pursuit neurons in the caudal frontal eye fields to motion-in-depth stimuli. *Exp Brain Res* 164:92–108.

- Alkan Y, Biswal BB, Alvarez TL. 2011a. Differentiation between vergence and saccadic functional activity within the human frontal eye fields and midbrain revealed through fMRI. *PLoS One* 6:e25866.
- Alkan Y, Biswal BB, Taylor PA, Alvarez TL. 2011b. Segregation of frontoparietal and cerebellar components within saccade and vergence networks using hierarchical independent component analysis of fMRI. *Vis Neurosci* 28:247–261.
- Alvarez TL, Alkan Y, Gohel S, Douglas Ward B, Biswal BB. 2010a. Functional anatomy of predictive vergence and saccade eye movements in humans: a functional MRI investigation. *Vis Res* 50:2163–2175.
- Alvarez TL, Bhavsar M, Semmlow JL, Bergen MT, Pedrono C. 2005. Short-term predictive changes in the dynamics of disparity vergence eye movements. *J Vis* 5:640–649.
- Alvarez TL, Semmlow JL, Yuan W, Munoz P. 2002. Comparison of disparity vergence system responses to predictable and non-predictable stimulations. *Curr Psychol Cogn* 21:243–261.
- Alvarez TL, Vicci VR, Alkan Y, Kim EH, Gohel S, Barrett AM, et al. 2010b. Vision therapy in adults with convergence insufficiency: clinical and functional magnetic resonance imaging measures. *Optom Vis Sci* 87:E985–E1002.
- Beckmann CF, Smith SM. 2004. Probabilistic independent component analysis for functional magnetic resonance imaging. *IEEE Trans Med Imaging* 23:137–152.
- Beckmann CF, Smith SM. 2005. Tensorial extensions of independent component analysis for multisubject fMRI analysis. *NeuroImage* 25:294–311.
- Behzadi Y, Restom K, Liu J, Liu TT. 2007. A component based noise correction method (CompCor) for BOLD and perfusion based fMRI. *Neuroimage* 37:90–101.
- Biswal B, Yetkin FZ, Haughton VM, Hyde JS. 1995. Functional connectivity in the motor cortex of resting human brain using echo-planar MRI. *Magn Reson Med* 34:537–541.
- Biswal BB, Mennes M, Zuo XN, Gohel S, Kelly C, Smith SM, et al. 2010. Toward discovery science of human brain function. *Proc Natl Acad Sci U S A* 107:4734–4739.
- Blautzik J, Keeser D, Berman A, Paolini M, Kirsch V, Mueller S, et al. 2012. Long-term test-retest reliability of resting-state networks in healthy elderly subjects and mild cognitive impairment patients. *J Alzheimers Dis* 34:741–754.
- Brannen JH, Badie B, Moritz CH, Quigley M, Meyerand ME, Haughton VM. 2001. Reliability of functional MR imaging with word-generation tasks for mapping Broca's area. *AJNR Am J Neuroradiol* 22:1711–1718.
- Breviglieri R, Hadjidimitrakis K, Bosco A, Sabatini SP, Galletti C, Fattori P. 2012. Eye position encoding in three-dimensional space: integration of version and vergence signals in the medial posterior parietal cortex. *J Neurosci* 32:159–169.
- Chen Y-F, Lee YY, Chen T, Semmlow JL, Alvarez TL. 2010. Behaviors, models and clinical applications of vergence eye movements. *J Med Biol Eng* 3:1–15.
- CITT. 2008. The convergence insufficiency treatment trial: design, methods, and baseline data. *Ophthalmic Epidemiol* 15:24–36.
- CITT. 2009. Long-term effectiveness of treatments for symptomatic convergence insufficiency in children. *Optom Vis Sci* 86:1096–1103.
- Cooper J, Jamal N. 2012. Convergence insufficiency—a major review. *Optometry* 83:137–158.
- Cooper JS, Burns CR, Cotter SA, Daum KM, Griffin JR, Scheiman MM. 2011. *Care of the Patient with Accommodative and Vergence Dysfunction*. St. Louis: American Optometric Association.
- Coubard OA, Kapoula Z. 2008. Saccades during symmetrical vergence. *Graefes Arch Clin Exp Ophthalmol* 246:521–536.
- Cox RW. 1996. AFNI: software for analysis and visualization of functional magnetic resonance neuroimages. *Comput Biomed Res* 29:162–173.
- Daum KM. 1984. Convergence insufficiency. *Am J Optom Physiol Opt* 61:16–22.
- Ferraina S, Brunamonti E, Giusti MA, Costa S, Genovesio A, Caminiti R. 2009. Reaching in depth: hand position dominates over binocular eye position in the rostral superior parietal lobule. *J Neurosci* 29:11461–11470.
- Ferraina S, Pare M, Wurtz RH. 2000. Disparity sensitivity of frontal eye field neurons. *J Neurophysiol* 83:625–629.
- Freyer T, Valerius G, Kuelz AK, Speck O, Glauche V, Hull M, et al. 2009. Test-retest reliability of event-related functional MRI in a probabilistic reversal learning task. *Psychiatry Res* 174:40–46.
- Fukushima K, Yamanobe T, Shinmei Y, Fukushima J, Kurkin S, Peterson BW. 2002. Coding of smooth eye movements in three-dimensional space by frontal cortex. *Nature* 419:157–162.
- Gamlin PD. 2002. Neural mechanisms for the control of vergence eye movements. *Ann N Y Acad Sci* 956:264–272.
- Gamlin PD, Yoon K. 2000. An area for vergence eye movement in primate frontal cortex. *Nature* 407:1003–1007.
- Gamlin PD, Yoon K, Zhang H. 1996. The role of cerebro-ponto-cerebellar pathways in the control of vergence eye movements. *Eye (Lond)* 10 (Pt 2):167–171.
- Genovesio A, Ferraina S. 2004. Integration of retinal disparity and fixation-distance related signals toward an egocentric coding of distance in the posterior parietal cortex of primates. *J Neurophysiol* 91:2670–2684.
- Geschwind N. 1970. The organization of language and the brain. *Science* 170:940–944.
- Gnadt JW, Mays LE. 1995. Neurons in monkey parietal area LIP are tuned for eye-movement parameters in three-dimensional space. *J Neurophysiol* 73:280–297.
- Golestani AM, Tymchuk S, Demchuk A, Goodyear BG. 2013. Longitudinal evaluation of resting-state fMRI after acute stroke with hemiparesis. *Neurorehabil Neural Repair* 27:153–163.
- Griffin JR. 1988. *Binocular Anomalies Procedures for Vision Therapy*. New York: Professional Press Books Fairchild Publications.
- Grisham JD. 1988. Visual therapy results for convergence insufficiency: a literature review. *Am J Optom Physiol Opt* 65:448–454.
- Hutchison RM, Gallivan JP, Culham JC, Gati JS, Menon RS, Everling S. 2012. Functional connectivity of the frontal eye fields in humans and macaque monkeys investigated with resting-state fMRI. *J Neurophysiol* 107:2463–2474.
- Jenkinson M, Bannister P, Brady M, Smith S. 2002. Improved optimization for the robust and accurate linear registration and motion correction of brain images. *NeuroImage* 17:825–841.
- Jenkinson M, Smith S. 2001. A global optimisation method for robust affine registration of brain images. *Med Image Anal* 5:143–156.
- Kapoula Z, Isotalo E, Muri RM, Bucci MP, Rivaud-Pechoux S. 2001. Effects of transcranial magnetic stimulation of the posterior parietal cortex on saccades and vergence. *Neuroreport* 12:4041–4046.
- Kapoula Z, Yang Q, Coubard O, Daunys G, Orssaud C. 2004. Transcranial magnetic stimulation of the posterior parietal

- cortex delays the latency of both isolated and combined vergence-saccade movements in humans. *Neurosci Lett* 360:95–99.
- Kapoula Z, Yang Q, Coubar O, Daunys G, Orssaud C. 2005. Role of the posterior parietal cortex in the initiation of saccades and vergence: right/left functional asymmetry. *Ann N Y Acad Sci* 1039:184–197.
- Kiehl KA, Liddle PF. 2003. Reproducibility of the hemodynamic response to auditory oddball stimuli: a six-week test-retest study. *Hum Brain Mapp* 18:42–52.
- Kim KH, Relkin NR, Lee KM, Hirsch J. 1997. Distinct cortical areas associated with native and second languages. *Nature* 388:171–174.
- Kim SG, Ogawa S. 2012. Biophysical and physiological origins of blood oxygenation level-dependent fMRI signals. *J Cereb Blood Flow Metab* 32:1188–1206.
- Kumar AN, Han Y, Garbutt S, Leigh RJ. 2002a. Properties of anticipatory vergence responses. *Invest Ophthalmol Vis Sci* 43:2626–2632.
- Kumar AN, Han Y, Ramat S, Leigh RJ. 2002b. Anticipatory saccadic-vergence responses in humans. *Ann N Y Acad Sci* 956:495–498.
- Laatsch L, Krisky C. 2006. Changes in fMRI activation following rehabilitation of reading and visual processing deficits in subjects with traumatic brain injury. *Brain Inj* 20:1367–1375.
- Laatsch LK, Thulborn KR, Krisky CM, Shobat DM, Sweeney JA. 2004. Investigating the neurobiological basis of cognitive rehabilitation therapy with fMRI. *Brain Inj* 18:957–974.
- Leavitt VM, Wylie GR, Girgis PA, Deluca J, Chiaravalloti ND. 2012. Increased functional connectivity within memory networks following memory rehabilitation in multiple sclerosis. *Brain Imaging Behav* [Epub ahead of print]; DOI: 10.1007/s11682-012-9183-2.
- Loubinoux I, Carel C, Alary F, Boulanouar K, Viillard G, Manelfe C, et al. 2001. Within-session and between-session reproducibility of cerebral sensorimotor activation: a test—retest effect evidenced with functional magnetic resonance imaging. *J Cereb Blood Flow Metab* 21:592–607.
- Lukasova K, Sommer J, Nucci-da-Silva MP, Vieira G, Blanke M, Bremmer F, et al. 2013. Test-retest reliability of fMRI activation generated by different saccade tasks. *J Magn Reson Imaging* [Epub ahead of print]; DOI: 10.1002/jmri.24369.
- Lund TE, Norgaard MD, Rostrup E, Rowe JB, Paulson OB. 2005. Motion or activity: their role in intra- and inter-subject variation in fMRI. *Neuroimage* 26:960–964.
- Margulies DS, Botter J, Long X, Lv Y, Kelly C, Schafer A, et al. 2010. Resting developments: a review of fMRI post-processing methodologies for spontaneous brain activity. *Magma* 23:289–307.
- Meindl T, Teipel S, Elmouden R, Mueller S, Koch W, Dietrich O, et al. 2010. Test-retest reproducibility of the default-mode network in healthy individuals. *Hum Brain Mapp* 31:237–246.
- Ming J, Thulborn KR, Szlyk JP. 2012. Reproducibility of activation maps for longitudinal studies of visual function by functional magnetic resonance imaging. *Invest Ophthalmol Vis Sci* 53:6153–6163.
- Nakamura T, Hillary FG, Biswal BB. 2009. Resting network plasticity following brain injury. *PLoS One* 4:e8220.
- Nitta T, Akao T, Kurkin S, Fukushima K. 2008a. Involvement of the cerebellar dorsal vermis in vergence eye movements in monkeys. *Cereb Cortex* 18:1042–1057.
- Nitta T, Akao T, Kurkin S, Fukushima K. 2008b. Vergence eye movement signals in the cerebellar dorsal vermis. *Prog Brain Res* 171:173–176.
- Parisi L, Rocca MA, Mattioli F, Copetti M, Capra R, Valsasina P, et al. 2013. Changes of brain resting state functional connectivity predict the persistence of cognitive rehabilitation effects in patients with multiple sclerosis. *Mult Scler* 20:686–694.
- Park CH, Chang WH, Ohn SH, Kim ST, Bang OY, Pascual-Leone A, et al. 2011. Longitudinal changes of resting-state functional connectivity during motor recovery after stroke. *Stroke* 42:1357–1362.
- Peelen MV, Downing PE. 2005. Within-subject reproducibility of category-specific visual activation with functional MRI. *Hum Brain Mapp* 25:402–408.
- Pickwell LD, Hampshire R. 1981. The significance of inadequate convergence. *Ophthalmic Physiol Opt* 1:13–18.
- Prevosto V, Graf W, Ugolini G. 2010. Cerebellar inputs to intraparietal cortex areas LIP and MIP: functional frameworks for adaptive control of eye movements, reaching, and arm/eye/head movement coordination. *Cereb Cortex* 20:214–228.
- Quinlan DJ, Culham JC. 2007. fMRI reveals a preference for near viewing in the human parieto-occipital cortex. *Neuroimage* 36:167–187.
- Raemaekers M, Bergsma DP, van Wezel RJ, van der Wildt GJ, van den Berg AV. 2011. Effects of vision restoration training on early visual cortex in patients with cerebral blindness investigated with functional magnetic resonance imaging. *J Neurophysiol* 105:872–882.
- Rouse MW, Borsting EJ, Mitchell GL, Scheiman M, Cotter SA, Cooper J, et al. 2004. Validity and reliability of the revised convergence insufficiency symptom survey in adults. *Ophthalmic Physiol Opt* 24:384–390.
- Sakata H, Taira M, Kusunoki M, Murata A, Tsutsui K, Tanaka Y, et al. 1999. Neural representation of three-dimensional features of manipulation objects with stereopsis. *Exp Brain Res* 128:160–169.
- Sander T, Sprenger A, Neumann G, Machner B, Gottschalk S, Rambold H, et al. 2009. Vergence deficits in patients with cerebellar lesions. *Brain* 132:103–115.
- Satterthwaite TD, Elliott MA, Gerraty RT, Ruparel K, Loughhead J, Calkins ME, et al. 2013. An improved framework for confound regression and filtering for control of motion artifact in the preprocessing of resting-state functional connectivity data. *Neuroimage* 64:240–256.
- Scheiman M, Gwiazda J, Li T. 2011. Non-surgical interventions for convergence insufficiency. *Cochrane Database Syst Rev* 3:CD006768.
- Scheiman M, Rouse M, Kulp MT, Cotter S, Hertle R, Mitchell GL. 2009. Treatment of convergence insufficiency in childhood: a current perspective. *Optom Vis Sci* 86:420–428.
- Scheiman M, Wick B. 2008. *Binocular Vision Heterophoric, Accommodative and Eye Movement Disorders*. Philadelphia: Lippincott Williams & Wilkins.
- Semmlow JL, Chen Y-F, Granger-Donetti B, Alvarez TL. 2009. Correction of saccade-induced midline errors in responses to pure disparity vergence stimuli. *J Eye Movement Res* 2:1–13.
- Semmlow JL, Chen Y-F, Pedrono C, Alvarez TL. 2008. Saccadic behavior during the response to pure disparity vergence stimuli I: general properties. *J Eye Movement Res* 1:1–11.
- Shaywitz SE, Shaywitz BA, Fulbright RK, Skudlarski P, Mencl WE, Constable RT, et al. 2003. Neural systems for compensation and persistence: young adult outcome of childhood reading disability. *Biol Psychiatry* 54:25–33.
- Shehzad Z, Kelly AM, Reiss PT, Gee DG, Gotimer K, Uddin LQ, et al. 2009. The resting brain: unconstrained yet reliable. *Cereb Cortex* 19:2209–2229.

- Smith SM. 2002. Fast robust automated brain extraction. *Hum Brain Mapp* 17:143–155.
- Song J, Desphande AS, Meier TB, Tudorascu DL, Vergun S, Nair VA, et al. 2012. Age-related differences in test-retest reliability in resting-state brain functional connectivity. *PLoS One* 7:e49847.
- Specht K, Willmes K, Shah NJ, Jancke L. 2003. Assessment of reliability in functional imaging studies. *J Magn Reson Imaging* 17:463–471.
- Taira M, Tsutsui KI, Jiang M, Yara K, Sakata H. 2000. Parietal neurons represent surface orientation from the gradient of binocular disparity. *J Neurophysiol* 83:3140–3146.
- Taubert M, Lohmann G, Margulies DS, Villringer A, Ragert P. 2011. Long-term effects of motor training on resting-state networks and underlying brain structure. *Neuroimage* 57:1492–1498.
- Tseng P, Chang CF, Chiau HY, Liang WK, Liu CL, Hsu TY, et al. 2013. The dorsal attentional system in oculomotor learning of predictive information. *Front Hum Neurosci* 7:404.
- Von Noorden GK, Campos EC. 2002. *Binocular Vision and Ocular Motility: Theory and Management of Strabismus*. St. Louis: Mosby.
- Yang Q, Kapoula Z. 2004. TMS over the left posterior parietal cortex prolongs latency of contralateral saccades and convergence. *Invest Ophthalmol Vis Sci* 45:2231–2239.
- Yetkin FZ, McAuliffe TL, Cox R, Haughton VM. 1996. Test-retest precision of functional MR in sensory and motor task activation. *AJNR Am J Neuroradiol* 17:95–98.
- Yoo SS, Wei X, Dickey CC, Guttman CR, Panych LP. 2005. Long-term reproducibility analysis of fMRI using hand motor task. *Int J Neurosci* 115:55–77.
- Zhang Y, Brady M, Smith S. 2001. Segmentation of brain MR images through a hidden Markov random field model and the expectation-maximization algorithm. *IEEE Trans Med Imaging* 20:45–57.
- Zou KH, Greve DN, Wang M, Pieper SD, Warfield SK, White NS, et al. 2005. Reproducibility of functional MR imaging: preliminary results of prospective multi-institutional study performed by biomedical informatics research network. *Radiology* 237:781–789.

Address correspondence to:

Tara L. Alvarez
Department of Biomedical Engineering
New Jersey Institute of Technology
University Heights
Newark, NJ 07102

E-mail: tara.l.alvarez@njit.edu

Bharat B. Biswal
Department of Biomedical Engineering
New Jersey Institute of Technology
University Heights
Newark, NJ 07102

E-mail: bharat.biswal@njit.edu